© 1998 The Chemical Society of Japan

Effects of Hydrogen Bonding and Hydrophobic Interactions on the Ultraviolet Resonance Raman Intensities of Indole Ring Vibrations

Motonori Matsuno and Hideo Takeuchi*

Pharmaceutical Institute, Tohoku University, Aobayama, Sendai 980-8578

(Received November 4, 1997)

UV resonance Raman intensities of indole ring vibrations were examined in solutions of different solvent properties to establish the correlation between the intensity and the environment of the indole ring, the main side-chain component of amino acid tryptophan. Each of the Raman bands that are enhanced through resonance with the B_b electronic transition gives the highest intensity when the indole NH site is hydrogen-bonded with a proton acceptor in hydrophobic environments. On the other hand, the Raman bands that gain intensity through resonance with the L_a transition are most enhanced when the indole ring is not hydrogen-bonded. Although these changes in Raman intensity result from small red and blue shifts of the B_b and L_a absorptions, respectively, the Raman intensity changes are much greater than the changes in UV absorption spectra. UV resonance Raman intensities are thus expected to be useful markers of hydrogen bonding and hydrophobic interactions of tryptophan residues in proteins.

Tryptophan (Trp) has the bulkiest side chain among the amino acids that occur in proteins. The main part of the Trp side chain is an indole ring, which carries an NH group on its hydrophobic aromatic ring. Hydrogen bonding at the NH site and hydrophobic interactions of the ring with its surroundings are both important factors that determine the role of a Trp residue in the structural stabilization and functioning of the protein.

Raman spectroscopy provides key information on the interactions of Trp residues in proteins. Previous studies have shown that the wavenumbers of ω4 (ca. 1490 cm^{-1}), ω6 (ca. 1430 cm^{-1}), and ω17 (ca. 880 cm^{-1}) Raman bands of the indole ring reflect the hydrogen bonding state at the NH site.[1,2] A correlation has been found between the intensity ratio of the ω7 Fermi doublet at 1360/1340 cm^{-1} and the strength of hydrophobic interaction of the indole ring.[3] The utility of these Raman bands as markers of hydrogen bonding and hydrophobic interactions has been demonstrated in visible and UV Raman studies on the structures of peptides and proteins.[1,4—12] Occasionally, however, the Raman marker bands are overlapped by other Raman bands and so they cannot be fully utilized.

In UV resonance Raman spectra, Raman bands gain intensity through resonance with one or more UV absorption bands, and the Raman intensity sensitively reflects changes of the resonant UV absorption bands, which might be caused by environmental changes such as hydrogen bonding and hydrophobic interactions. The indole ring has three UV absorption bands in the 200—300 nm region and Raman excitation in this wavelength region produces strong Raman scattering.[13—16] The intensities of UV resonance Raman bands of the indole ring are thus potential markers of the hydrogen bonding at the NH site and/or hydrophobic interactions of the indole aromatic ring. Previously, it was reported that certain Raman bands of Trp excited at 230 or 240 nm showed large intensity increases associated with environmental changes.[4,8,17] The observed intensity increase was ascribed to an increased resonance effect resulting from a red shift of the B_b absorption band at ca. 220 nm.[4,8] However, detailed relationships between the environment and UV resonance Raman intensity have not yet been elucidated.

In this study, we have conducted a systematic investigation of the effects of hydrogen bonding and hydrophobic interactions on the UV resonance Raman bands of the indole ring by using 3-methylindole (skatole), a model compound for Trp, dissolved in solvents with different hydrogen-bonding and hydrophobic/hydrophilic properties. UV resonance Raman scattering was excited at several wavelengths in the 230—270 nm region and the intensities of Raman bands were measured as a function of excitation wavelength. Comparison of the excitation profiles observed in different solvents has shown that the Raman bands that are enhanced through resonance with the B_b transition become strongest when the indole ring is hydrogen-bonded in hydrophobic environments. On the other hand, the Raman bands that are enhanced via resonance with the L_a transition, give the highest intensity when the indole NH site is not involved in hydrogen bonding. A further detailed examination of the effects of hydrogen bonding has revealed a few Raman bands whose intensities and wavenumbers serve as possible markers of hydrogen bonding.

Experimental

Skatole, methanol, 1-butanol (hereafter abbreviated butanol), cyclohexane, and hexamethylphosphoric triamide (HMPA) were purchased from Nacalai Tesque. Hexane of HPLC grade and sodium perchlorate ($NaClO_4$) were purchased from Kanto Kagaku Co. H_2O was distilled and deionized on an ion-exchange column.

Raman spectra were recorded in a 180° back-scattering geometry on a fore-prism UV Raman spectrometer (JASCO TR-600UV)[18] equipped with a CCD detector (Princeton Instruments) of 576 pixels (ICCD-576) or 1152 pixels (LN/CCD-1152). Excitation was effected by the following two laser systems: (a) a dye laser (Lambda Physik FL3002) pumped by a pulsed XeCl excimer laser (Lambda Physik LPX240i), which was used to obtain frequency-doubled UV pulses at 235, 240, 245, 250, 255, 260, 263, and 267 nm (repetition rate 200 Hz, average power 0.6—1.2 mW) and (b) an intra-cavity frequency-doubled Ar ion laser (Coherent Innova 300 FReD) from which continuous-wave (CW) radiation of 229 or 257 nm (2—4 mW) was obtained. Saturation of Raman intensity due to ground-state depletion[19,20] was negligibly small under the pulse excitation conditions employed here[21] and could not occur for the CW excitation. Since the pulse laser system provided a wider range of wavelength tuning than the CW laser system, we used the pulse laser for recording Raman excitation profiles. The CW laser was used for a detailed examination of the effects of hydrogen bonding.

To obtain Raman excitation profiles, an aqueous solution of skatole was prepared at a concentration of 1 mM (1 M = 1 mol dm^{-3}). Skatole was also dissolved in methanol, butanol, and cyclohexane at 5 mM concentration. $NaClO_4$ was added to the aqueous and methanol solutions at concentrations of 100 and 500 mM, respectively. Intensities of Raman bands of skatole in aqueous and methanol solutions were measured relative to the peak intensity of the 933 cm^{-1} band of ClO_4^-. It is known that ClO_4^- is an ideal standard for Raman intensity measurements in the UV spectral region.[22] For butanol and cyclohexane solutions, solvent Raman bands were used as intensity references because $NaClO_4$ was insoluble in these solvents. To determine the Raman intensities of butanol and cyclohexane, we first determined the relative intensity of the 1032 cm^{-1} band of methanol with respect to the ClO_4^- 933 cm^{-1} band. Then, the intensities of the 1299 cm^{-1} band of butanol and the 1266 cm^{-1} band of cyclohexane relative to that of the ClO_4^- band were evaluated from Raman spectra of binary mixtures of solvents by using the methanol 1032 cm^{-1} band as a secondary intensity standard. The determination of solvent Raman intensities was performed at every Raman excitation wavelength employed here.

For examination of the effects of hydrogen bonding, Raman spectra were excited at 229 and 257 nm. Skatole was dissolved in hexane (1 and 5 mM for 229 and 257 nm excitation, respectively) and a small amount of HMPA was added to the solution. The hydrogen-bonding state of skatole was monitored by recording infrared spectra in the N–H stretching region. The Raman bands of solvent hexane were used as intensity references to compare the Raman intensities of indole ring vibrations in the absence and presence of hydrogen bonding.

UV absorption spectra of skatole in solutions (concentration 0.05—0.10 mM) were recorded on a Hitachi 220A spectrophotometer with a 1 mm cell. Infrared spectra were recorded on a Hitachi IR-7000 Fourier-transform spectrometer.

Results and Discussion

Solvent Effects on UV Absorption Spectra. Figure 1 shows UV absorption spectra of skatole dissolved in solvents with different hydrogen-bonding and hydrophobic/hydrophilic properties: cyclohexane (non-hydrogen-bonding and hydrophobic), butanol (hydrogen-bonding and hydrophobic), methanol (hydrogen-bonding and weakly hydrophobic), and H_2O (hydrogen-bonding and hydrophilic). In the wavelength region examined (210—310 nm), the B_b transition gives the strongest absorption. The wavelength of absorption maximum (λ_{max}) of the B_b band is located at 220.4 nm in H_2O solution. In cyclohexane solution, the λ_{max} does not change from that of aqueous solution, but the extinction coefficient at λ_{max} becomes larger by about 10% with a slight decrease in bandwidth. Hydrophobic interactions seem to increase the peak absorption intensity. Significant red shifts of the λ_{max} are observed for methanol (1.4 nm) and butanol solutions (2.6 nm), with concomitant increases in extinction coefficient in this order. Since the proton accepting ability of the solvent in hydrogen bonding is in the order butanol > methanol$\gg H_2O$,[23] the red shift correlates with the strength of hydrogen bonding at the indole NH site. (The NH stretching band of skatole was covered by a much stronger OH stretching band of the solvent and could not be detected in infrared and Raman spectra.) Hydrogen bonding in hydrophobic environments is most effective in causing the red shift and intensity increase of the B_b absorption band.

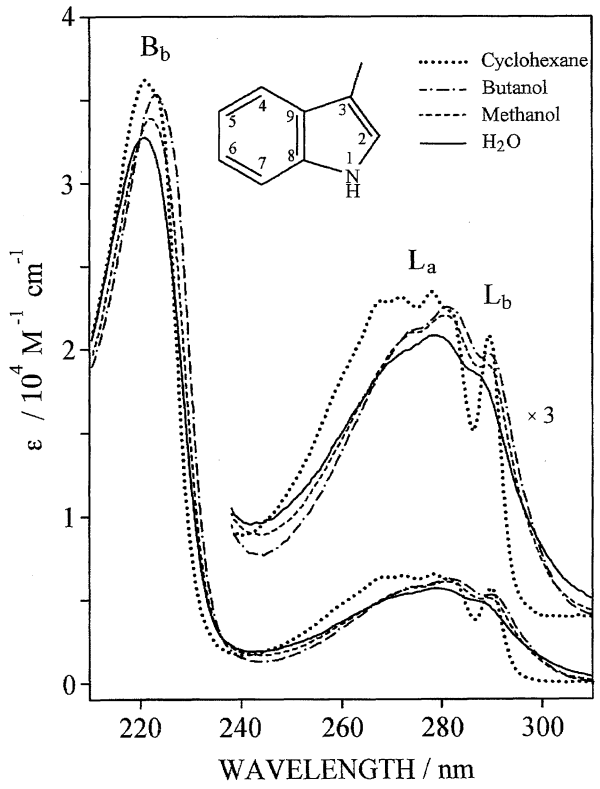

Fig. 1. UV absorption spectra of skatole in cyclohexane, butanol, methanol, and H_2O solutions.

In the 250—300 nm region, a broad feature is observed for H_2O solution. This is due to an overlap of the stronger L_a (ca. 275 nm) and weaker L_b (ca. 290 nm) transitions.[24,25] On going from H_2O solution to methanol or butanol solution, both the L_a and L_b bands shift to the red by 1—3 nm. In cyclohexane solution, on the other hand, the L_a band largely shifts to the blue, while the L_b band remains almost unshifted. The significant blue shift of the L_a absorption in non-hydrogen-bonding solutions and the relative insensitivity of the L_b band to solvent properties are consistent with the results of previous solvent effect studies on indole derivatives.[25,26]

Since the L_a band shows a further blue shift on going from non-hydrogen-bonding solution to the vapor phase,[25] hydrophobic interactions seem to be a factor to shift the L_a band to the red. Accordingly, the blue shift of the L_a band in cyclohexane solution is ascribed solely to the absence of hydrogen bonding.

Solvent Effects on UV Resonance Raman Intensity. We have examined UV resonance Raman spectra of skatole in cyclohexane, butanol, methanol, and H_2O solutions by using excitation wavelengths of 235, 240, 245, 250, 255, 260, 263, and 267 nm. Figures 2 and 3 show the spectra excited at 235 and 260 nm, respectively. With 235 nm excitation, strong Raman scattering is observed for the $\omega 1$ (ca. 1620 cm^{-1}), $\omega 3$ (ca. 1560 cm^{-1}), $\omega 7$ (ca. 1350 cm^{-1}), and $\omega 16$ (ca. 1010 cm^{-1}) modes. These vibrations except $\omega 1$ are known to gain intensity from the B_b transition.[21,27] The intensity of the $\omega 1$ band mainly comes from the B_a transition, which is located at a shorter wavelength (ca. 195 nm).[21] The Fermi doublet of $\omega 7$ is not well resolved in the spectra because of a small separation of the doublet in skatole.[3] With 260 nm excitation, the $\omega 1$ (ca. 1620 cm^{-1}) and $\omega 2$ (ca. 1580 cm^{-1}) bands are selectively enhanced as shown in Fig. 3. The other bands including the $\omega 3$, $\omega 7$, and $\omega 16$ bands are not much enhanced. The selective enhancement of the $\omega 1$ and $\omega 2$ bands was also observed in UV resonance Raman spectra of aqueous Trp excited at 260 and 279 nm.[27]

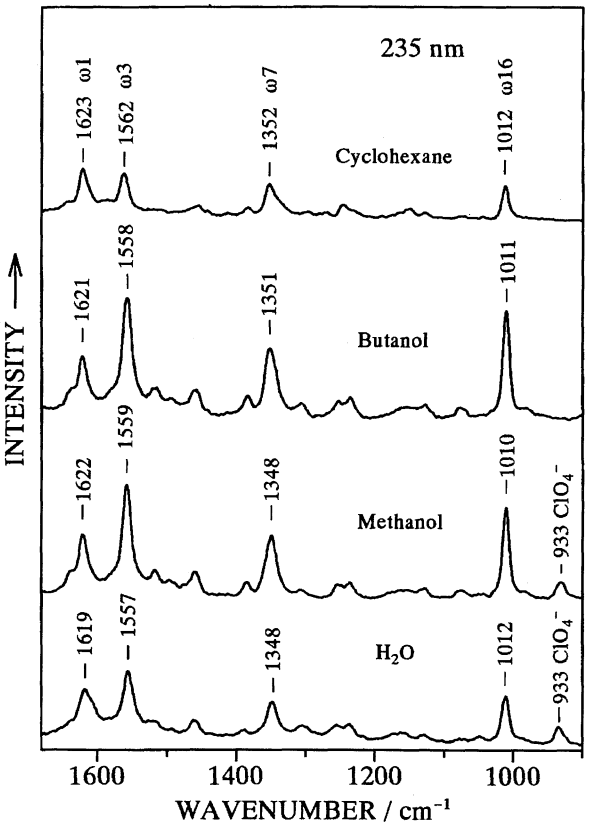

Fig. 2. Comparison of 235-nm-excited resonance Raman spectra of skatole in cyclohexane, butanol, methanol, and H_2O solutions. The intensity was calibrated with the 933 cm^{-1} band of ClO_4^- added as an internal intensity standard (methanol and H_2O solutions) or with the solvent Raman bands whose intensities were determined separately as described in text (cyclohexane and butanol solutions). Solvent Raman bands were subtracted from the spectra after the intensity calibration.

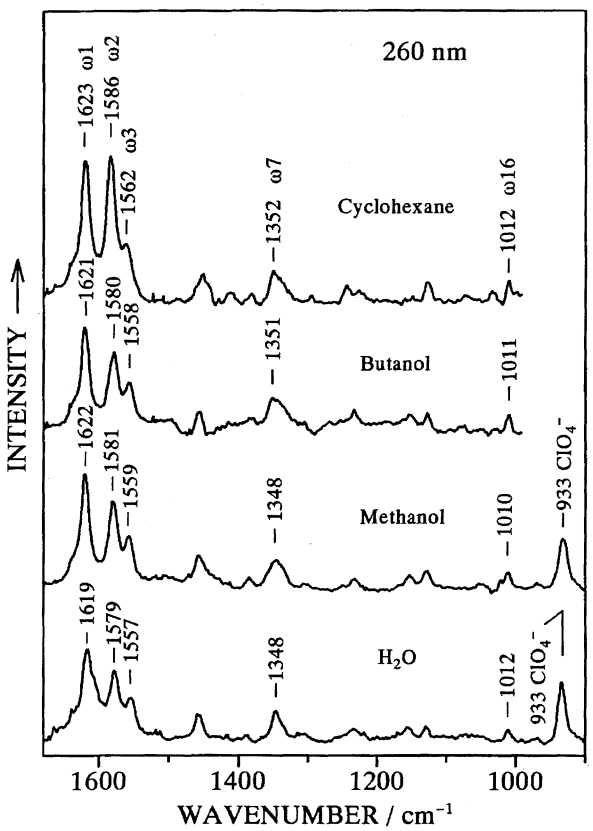

Fig. 3. Comparison of 260-nm-excited resonance Raman spectra of skatole in cyclohexane, butanol, methanol, and H_2O solutions. The intensity was calibrated with the 933 cm^{-1} band of ClO_4^- added as an internal intensity standard (methanol and H_2O solutions) or with the solvent Raman bands whose intensities were determined separately as described in text (cyclohexane and butanol solutions). Solvent Raman bands were subtracted from the spectra after the intensity calibration.

The UV resonance Raman intensities of the $\omega 1$, $\omega 3$, $\omega 7$, and $\omega 16$ bands are plotted as a function of the excitation wavelength in Fig. 4. In these excitation profiles, the peak intensity of a Raman band is displayed as a relative value with respect to that of the 933 cm^{-1} band of equimolar ClO_4^-. The $\omega 1$ band is moderately intense in the 240—270 nm region and becomes stronger when excited at 235 nm. This is because the $\omega 1$ band is mainly enhanced by preresonance with the B_a transition and the effect of resonance with the B_b transition becomes prominent only when the excitation wavelength is very close to or within the B_b absorption band. The overlapping contributions from the B_a and B_b transitions make the solvent dependence of the $\omega 1$ intensity somewhat complicated. In the wavelength region where the B_b preresonance effect is dominant ($\geq$ 240 nm), the $\omega 1$ band is a little stronger in hydrophobic environments (cyclohexane) than in

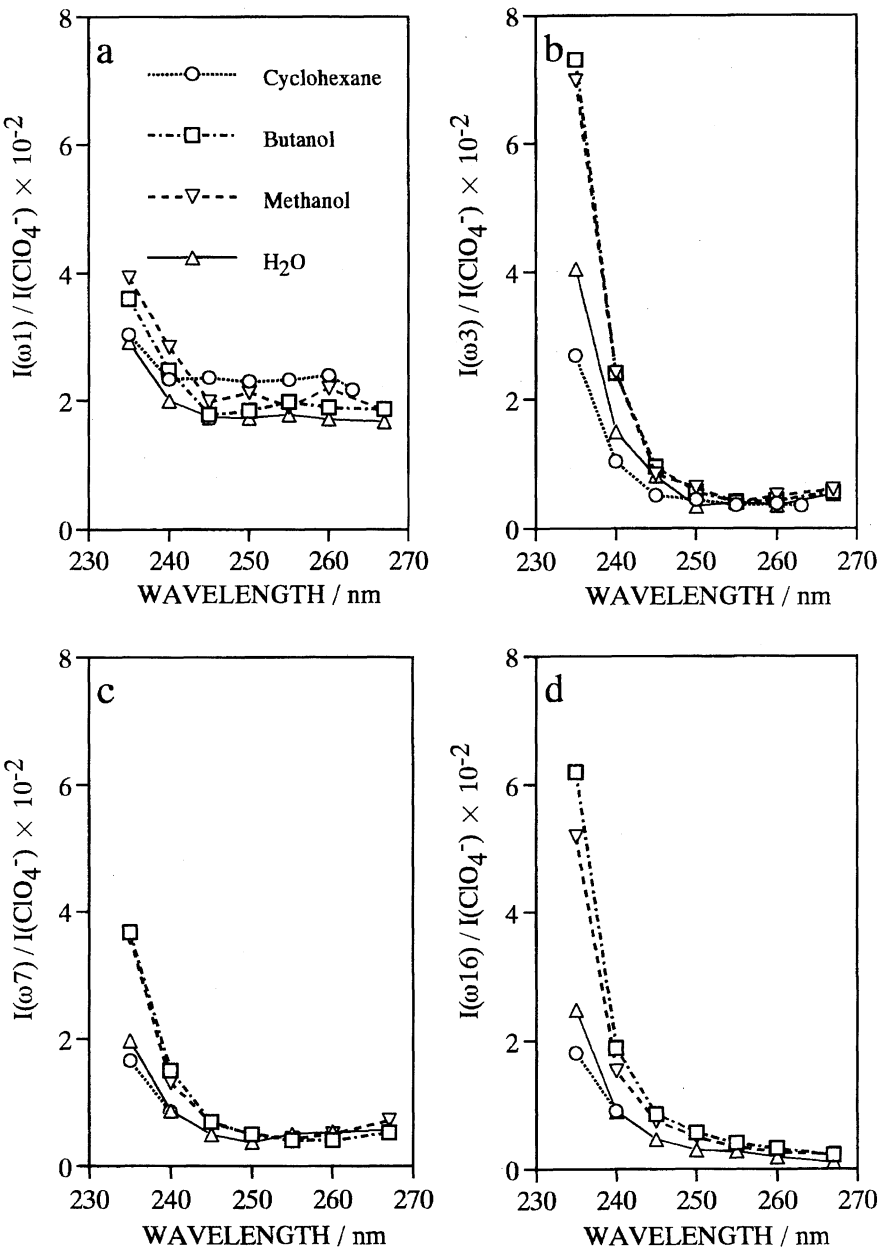

Fig. 4. Excitation profiles for the (a) $\omega1$, (b) $\omega3$, (c) $\omega7$, and (d) $\omega16$ Raman bands of skatole in cyclohexane, butanol, methanol, and H_2O solutions. The intensity is displayed as a relative value with respect to that of the 933 cm^{-1} band of equimolar ClO_4^-.

hydrophilic environments (H_2O). On the other hand, when the B_b resonance effect is significant, such as in the spectra excited at 235 nm, the $\omega1$ band is slightly more enhanced in hydrogen-bonding and hydrophobic solvents (methanol and butanol) than in the other solvents (cyclohexane and H_2O). Although the $\omega1$ intensity is affected by the solvent as described above, the intensity change is no more than 35%. The $\omega1$ band may be used as an intensity reference when other intensity standards are not available.

The excitation profiles of the $\omega3$, $\omega7$, and $\omega16$ bands in Fig. 4 show that these Raman bands gain intensity through resonance with the B_b transition but not through preresonance with the B_a transition. The solvent effects on the excitation profiles of these Raman bands are therefore simpler than those on the $\omega1$ excitation profile. Generally, the Raman bands of $\omega3$, $\omega7$, and $\omega16$ are stronger in methanol and butanol than in cyclohexane and H_2O, and the intensity ratio between the two groups of solvents becomes 2—4 when excited at 235 nm. The large solvent dependence of the Raman intensity at shorter wavelengths is consistent with the red shift and intensification of the B_b absorption band observed in the former group of solvents. It is interesting to note that UV Raman bands recorded under B_b resonance conditions show significant intensification only in the presence of both hydrogen bonding and hydrophobic interactions. The $\omega3$, $\omega7$, and $\omega16$ intensities may be used to detect the hydrogen bonding at the NH site of Trp located in hydrophobic environments.

Figure 5 shows the excitation profile of the $\omega2$ band, which is largely enhanced through resonance with the L_a transition.

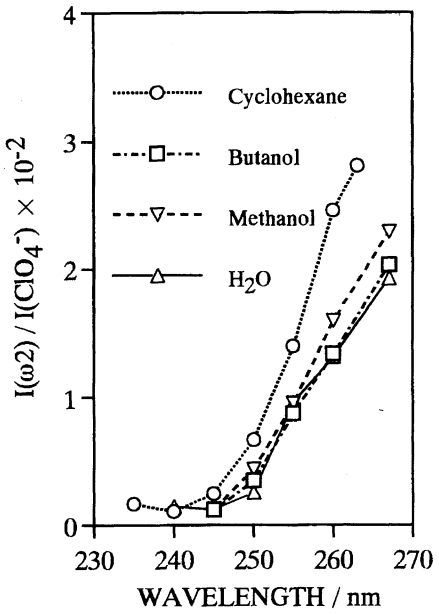

Fig. 5. Excitation profile for the $\omega2$ Raman band of skatole in cyclohexane, butanol, methanol, and H_2O solutions. The intensity is displayed as a relative value with respect to that of the 933 cm^{-1} band of equimolar ClO_4^-.

When the excitation wavelength is close to or within the L_a absorption band (250—270 nm), the $\omega2$ band is much stronger in cyclohexane than in the hydrogen-bonding solvents (H_2O, methanol, and butanol). The specific intensification of the $\omega2$ band in cyclohexane is consistent with the blue shift of the L_a absorption band in this solvent. The excitation profile of the $\omega2$ band closely traces the change of the L_a absorption band in different solvents (compare Figs. 1 and 5). This observation proves that the $\omega2$ band gains intensity from the L_a transition if the excitation wavelength lies in the 250—270 nm region. If the L_b transition, whose λ_{max} is insensitive to solvent properties, significantly contributed to the Raman intensity of $\omega2$, the $\omega2$ intensity would not have shown such a large solvent dependence. The L_a-resonant Raman bands are thus expected to become stronger upon disruption of a hydrogen bond. The intensification of the $\omega2$ Raman band may be regarded as a marker of the non-hydrogen-bonded state of Trp when the protein is excited at 250—270 nm.

Effects of Hydrogen Bonding. Trp residues are sometimes buried in the hydrophobic interior of the protein and are hydrogen-bonded with other amino acid side-chains or with water molecules trapped in proteinous cavities. The strength of hydrogen bonding varies or the hydrogen bond disrupts upon conformational change of the protein in the process of protein functioning. The present solvent effect study has shown that the B_b-resonant Raman bands such as $\omega3$, $\omega7$, and $\omega16$ would give high intensities when the indole ring of Trp is interacting with its hydrophobic surroundings and the indole NH site is hydrogen bonded with a proton acceptor. In the same state of Trp, the L_a-resonant Raman bands such as $\omega2$ are expected to be weak and to gain intensity upon disruption of the hydrogen bond. To elucidate the effects of hydrogen bonding in hydrophobic environments in more detail, we have examined UV resonance Raman spectra in a wider wavenumber range with a higher spectral resolution and a higher signal-to-noise ratio by using the LN/CCD detector and the CW UV laser described in Experimental section.

Figures 6 and 7 show resonance Raman spectra of skatole excited at 229 (resonant with B_b) and 257 nm (resonant with L_a), respectively. Skatole was dissolved in hexane in the absence (trace a in each figure) and presence (trace b) of a small amount (ca. 0.1% v/v against hexane) of HMPA, a strong proton acceptor.[23] Infrared spectra showed that about 60% of skatole molecules are hydrogen-bonded in the presence of HMPA. (A minimal amount of HMPA was added to avoid change in hydrophobic interaction.) The bottom trace (c) in each figure shows the difference spectrum, b—a. The positive peaks in the difference spectrum indicate that intensity increases upon hydrogen bonding.

With 229 nm excitation (Fig. 6), the $\omega3$, $\omega7$, and $\omega16$

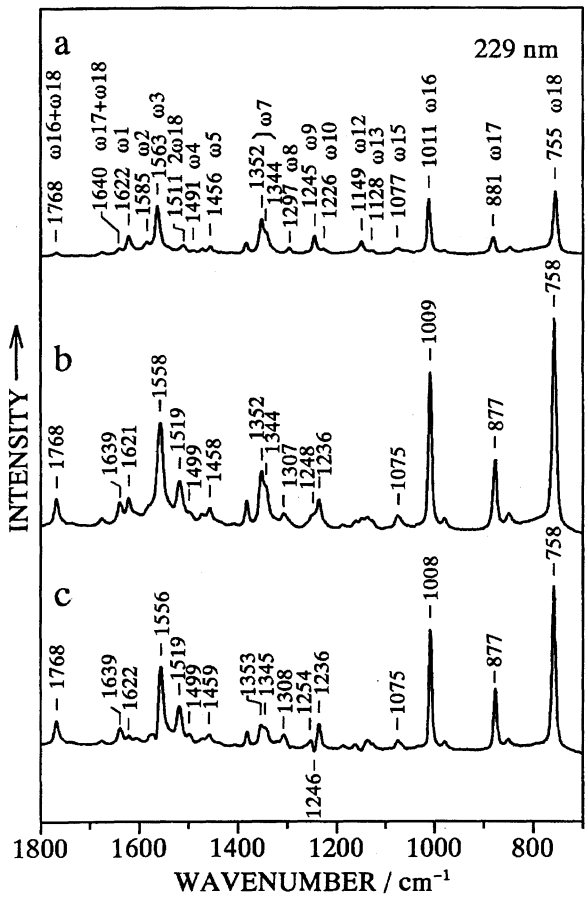

Fig. 6. Raman spectra of skatole excited at 229 nm: (a) hexane solution, (b) hexane solution containing a trace amount (0.08%, v/v) of hexamethylphosphoric triamide (a strong hydrogen bonding acceptor), and (c) the difference spectrum, b—a, showing the effects of hydrogen bonding. The skatole concentration was 1 mM. The intensity was calibrated with the Raman bands of solvent hexane and then the solvent Raman bands were subtracted.

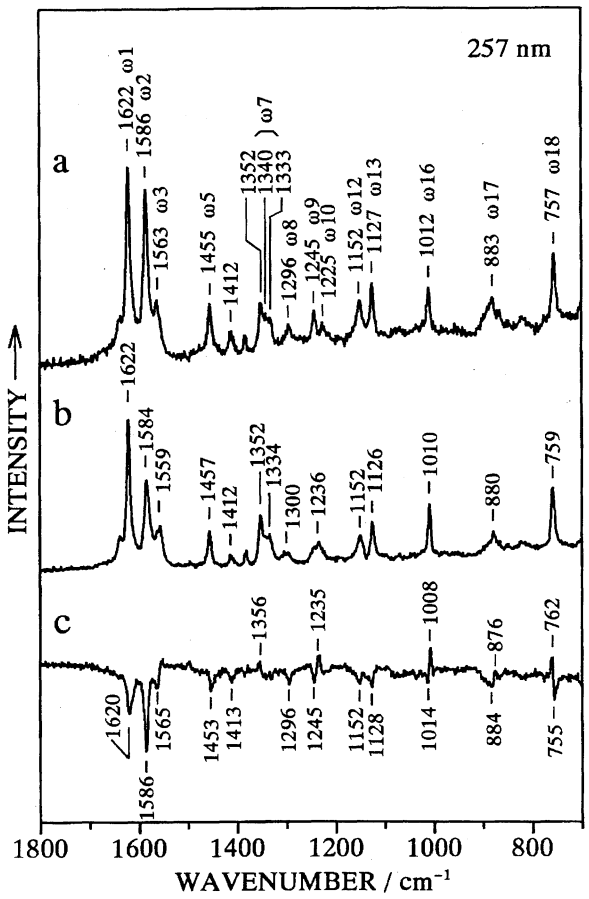

Fig. 7. Raman spectra of skatole excited at 257 nm: (a) hexane solution, (b) hexane solution containing a trace amount (0.12%, v/v) of hexamethylphosphoric triamide (a strong hydrogen bonding acceptor), and (c) the difference spectrum, b—a, showing the effects of hydrogen bonding. The skatole concentration was 5 mM. The intensity was calibrated with the Raman bands of solvent hexane and then the solvent Raman bands were subtracted.

bands give prominent positive peaks in the difference spectrum as expected. Likewise, the $\omega 17$ (ca. 880 cm^{-1}) and $\omega 18$ (ca. 755 cm^{-1}) bands, which are also B_b-resonant,[21,27] show significant intensity increases. The intensities of these fundamental bands are good markers of hydrogen bonding. A new feature revealed by these spectra is the intensity increase and wavenumber shift of a band at 1510—1520 cm^{-1}, which is assigned to the overtone of $\omega 18$ (2ω 18).[8] The intensity increase of $2\omega 18$ is proportional to that of the fundamental $\omega 18$, and the wavenumber shift of $2\omega 18$ (from 1511 to 1519 cm^{-1}) is about twice that of $\omega 18$ (from 755 to 758 cm^{-1}). According to the Raman spectra reported for Trp derivatives in the crystalline state,[2] the $\omega 18$ wavenumber is 756±1 and 759±1 cm^{-1} when the indole N–H stretching wavenumber is above (weakly hydrogen-bonded) and below 3400 cm^{-1} (strongly hydrogen-bonded), respectively. Although the change of the $\omega 18$ wavenumber is too small to be used as a marker of hydrogen bonding, the wavenumber difference (8 cm^{-1}) of $2\omega 18$ between the hydrogen-bonded and non-hydrogen-bonded states is large enough to be distinguished. Accordingly, both the intensity and wavenumber of $2\omega 18$ may be used to monitor the hydrogen bonding at the indole NH site. A significant intensity increase of the $2\omega 18$ band has been observed to occur upon structural transition from the CO-ligated to unligated state of hemoglobin in 230-nm-excited resonance Raman spectra.[8,28]

The band at 1768 cm^{-1} in Fig. 6 is assigned to the combination $\omega 16+\omega 18$.[27] The intensity of this band increases with hydrogen bonding. Likewise, the 1640 cm^{-1} band assignable to the combination $\omega 17+\omega 18$ increases in intensity. The wavenumbers of these combination bands do not appear to change because the upshift of one component ($\omega 18$) upon hydrogen bonding is compensated by the corresponding downshift of the other component ($\omega 16$ or $\omega 17$). The $\omega 16+\omega 18$ band is located in a window region of UV resonance Raman spectra of proteins and it would not be overlapped by other Raman bands. Actually, a band of moderate intensity assignable to $\omega 16+\omega 18$ has been observed in a 229-nm-excited Raman spectrum of bacteriophage *fd*, which contains one Trp residue in each of the 2700 copies of 50-residue coat protein subunit.[29] The intensity of this combination band is thus expected to be a useful hydrogen bonding marker. On the other hand, the $\omega 17+\omega 18$ band may not be useful because its intensity increase is rather small and the band would be covered by the tail of a tyrosine Raman band at 1616 cm^{-1}, which is also enhanced with excitation around 230 nm.[21,27]

Another interesting feature in Fig. 6 is the intensification of $\omega 10$ upon hydrogen bonding. Concomitant with the intensity increase, this band shifts from 1226 to 1236 cm^{-1}, which is accompanied by a small (3 cm^{-1}) upshift of the neighboring $\omega 9$ band. The $\omega 8$ band at 1297 cm^{-1} also intensifies and shifts by +10 cm^{-1} upon hydrogen bonding, though the intensity increase of $\omega 8$ is smaller than that of $\omega 10$. The $\omega 8$, $\omega 9$, and $\omega 10$ bands are relatively weak but still observable in protein Raman spectra if the excitation wavelength is around 230 nm.[8,29] The intensities and wavenumbers of these Raman bands, in particular of $\omega 10$, may serve as markers of hydrogen bonding.

With 257 nm excitation, only the $\omega 1$ and $\omega 2$ bands show significant intensity changes upon hydrogen bonding (Fig. 7). The intensity decrease of $\omega 2$ is much larger than that of $\omega 1$ and the intensity ratio $I(\omega 2)/I(\omega 1)$ changes from ca. 0.9 to ca. 0.6 upon formation of a hydrogen bond at the indole NH site. The $I(\omega 2)/I(\omega 1)$ ratio may be used to monitor the hydrogen bonding as proposed previously.[4]

The $\omega 2$ mode is unique among the indole ring vibrations in its specific resonance with the L_a transition. According to a normal coordinate calculation on the indole ring,[30] the $\omega 2$ mode is an in-phase stretching vibration of the C_4–C_9 and C_6–C_7 bonds (for atom numbering, see Fig. 1). The atomic displacements in the $\omega 2$ vibration may be closely related to the geometrical change of the indole ring upon L_a transition but not upon B_b nor L_b transition, resulting in a strong coupling of the $\omega 2$ vibration with the L_a electronic transition and in the L_a-specific resonance Raman enhancement of $\omega 2$.[31] A molecular orbital calculation study has

predicted that the L_a transition causes shortening of both the C_4–C_9 and C_6–C_7 bonds, but the L_b transition does not.[32] No other vibrations of the indole ring involve in-phase stretching of the C_4–C_9 and C_6–C_7 bonds.[30] This may be the reason why the $\omega 2$ band alone shows the L_a-specific resonance enhancement. The unique property of the $\omega 2$ band has been exploited in determining the direction of the L_a transition moment from its Raman intensity in polarized UV resonance Raman spectra.[33]

In this study, we have examined the resonance Raman intensities of indole ring vibrations and their dependence on the environment by using excitation wavelengths in the 230—270 nm region, where UV resonance Raman spectra of proteins are usually excited. The results have shown that the intensities of B_b-resonant Raman bands become stronger upon formation of a hydrogen bond at the indole NH site, while the other part of indole ring is interacting with hydrophobic surroundings. On the other hand, the L_a-resonant Raman bands are most enhanced when the indole ring is not hydrogen-bonded. The correlations between the UV resonance Raman intensity and the environment of the indole ring are expected to be useful in studying the hydrogen bonding states and hydrophobic interactions of Trp residues in proteins.

References

1) T. Miura, H. Takeuchi, and I. Harada, *Biochemistry*, **27**, 88 (1988).

2) T. Miura, H. Takeuchi, and I. Harada, *J. Raman Spectrosc.*, **20**, 667 (1989).

3) I. Harada, T. Miura, and H. Takeuchi, *Spectrochim. Acta, Part A*, **42**, 307 (1986).

4) I. Harada, T. Yamagishi, K. Uchida, and H. Takeuchi, *J. Am. Chem. Soc.*, **111**, 8926 (1989).

5) H. Takeuchi, Y. Nemoto, and I. Harada, *Biochemistry*, **29**, 1572 (1990).

6) S. Kaminaka, T. Ogura, and T. Kitagawa, *J. Am. Chem. Soc.*, **112**, 23 (1990).

7) T. Miura, H. Takeuchi, and I. Harada, *Biochemistry*, **30**, 6074 (1991).

8) K. R. Rodgers, C. Su, S. Subramaniam, and T. G. Spiro, *J. Am. Chem. Soc.*, **114**, 3697 (1992).

9) S. Hashimoto, T. Yabusaki, H. Takeuchi, and I. Harada, *Biospectroscopy*, **1**, 375 (1995).

10) M. Nagai, S. Kaminaka, Y. Ohba, Y. Nagai, Y. Mizutani, and T. Kitagawa, *J. Biol. Chem.*, **270**, 1636 (1995).

11) S. A. Overman and G. J. Thomas, Jr., *Biochemistry*, **34**, 5440 (1995).

12) S. Hashimoto, K. Obata, H. Takeuchi, R. Needleman, and J. K. Lanyi, *Biochemistry*, **36**, 11583 (1997).

13) R. P. Rava and T. G. Spiro, *J. Phys. Chem.*, **89**, 1586 (1985).

14) S. A. Asher, M. Ludwig, and C. R. Johnson, *J. Am. Chem. Soc.*, **108**, 3186 (1986).

15) I. Harada and H. Takeuchi, "Spectroscopy of Biological Systems, Advances in Spectroscopy," ed by R. J. H. Clark and R. E. Hester, Wiley, Chichester (1986), Vol. 13, Chap. 3.

16) J. C. Austin, T. Jordan, and T. G. Spiro, "Biomolecular Spectroscopy Part A, Advances in Spectroscopy," ed by R. J. H. Clark and R. E. Hester, Wiley, Chichester (1993), Vol. 20, Chap. 2.

17) R. G. Efremov, A. V. Feofanov, and I. R. Nabiev, *J. Raman Spectrosc.*, **23**, 69 (1992).

18) S. Hashimoto, T. Ikeda, H. Takeuchi, and I. Harada, *Appl. Spectrosc.*, **47**, 1283 (1993).

19) S. Krimm, S. Song, and S. A. Asher, *J. Am. Chem. Soc.*, **111**, 4290 (1989).

20) S. Song and S. A. Asher, *J. Am. Chem. Soc.*, **111**, 4295 (1989).

21) C. Su, Y. Wang, and T. G. Spiro, *J. Raman Spectrosc.*, **21**, 435 (1990).

22) D. M. Dudik, C. R. Johnson, and S. A. Asher, *J. Phys. Chem.*, **82**, 1732 (1985).

23) M. J. Kamlet and R. W. Taft, *J. Am. Chem. Soc.*, **98**, 377 (1976).

24) G. Weber, *Biochem. J.*, **75**, 335 (1960).

25) E. H. Strickland, J. Horwitz, and C. Billups, *Biochemistry*, **9**, 4914 (1970).

26) E. H. Strickland, C. Billups, and E. Kay, *Biochemistry*, **11**, 3657 (1972).

27) J. A. Sweeney and S. A. Asher, *J. Phys. Chem.*, **94**, 4784 (1990).

28) S. Huang, E. S. Peterson, C. Ho, and J. M. Friedman, *Biochemistry*, **36**, 6197 (1997).

29) Z. Q. Wen, S. A. Overman, and G. J. Thomas, Jr., *Biochemistry*, **36**, 7810 (1997).

30) H. Takeuchi and I. Harada, *Spectrochim. Acta, Part A*, **42**, 1069 (1986).

31) A. C. Albrecht, *J. Chem. Phys.*, **34**, 1476 (1961).

32) P. R. Callis, *J. Chem. Phys.*, **95**, 4230 (1991).

33) H. Takeuchi, M. Matsuno, S. A. Overman, and G. J. Thomas, Jr., *J. Am. Chem. Soc.*, **118**, 3498 (1996).